Nitrogen Cycling

https://doi.org/10.48130/nc-0026-0004

Original Research

Open Access

Bacterial rather than fungal denitrification as a key driver for increased denitrification rate under warming in paddy soil

Lixin Jia[1,2], Yong Li[3*], Roland Bol[4,5] and Di Wu[2*]

Received: 12 November 2025

Revised: 22 January 2026

Accepted: 13 March 2026

Published online: 31 March 2026

Abstract

Biological denitrification, carried out by both bacteria and fungi, is a major pathway contributing to nitrous oxide (N_2O) emissions in paddy soil due to active denitrification under fluctuating redox conditions. However, warming-induced shifts in fungal and bacterial contributions to denitrification-derived N_2O emissions in paddy soil remain unclear. Using eighteen paddy soils distributed along a latitudinal gradient in China (19°53′ N–45°31′ N), this study examined the response of potential denitrification-derived N_2O emissions to experimental warming (+4 °C). Using the N_2O site preference approach, we further distinguished the differential responses of bacterial and fungal denitrification to warming. Results showed that the temperature response ratios of denitrification potential varied among sites from 0.04 to 0.21, with the response being closely associated with bacterial denitrification. Under 4 °C warming, the relative contribution of bacterial denitrification increased from 53% to 59%, whereas that of fungal denitrification decreased from 47% to 41%. Bacterial denitrification rate was positively linked to *nirS*, whereas fungal denitrification rate was tightly coupled to *FnirK*, *nosZII*, and *nirS* abundance. Structural equation modeling revealed soil nutrient dynamics and functional gene expression. These insights lead us to a more nuanced understanding of microbial-driven N_2O emissions in paddy soils under warming, emphasizing the need for region-specific, microbe-targeted strategies to predict and mitigate N_2O emissions in the context of global warming.

Keywords: Denitrification potential rate, Fungal denitrification, Bacterial denitrification, Warming, Paddy soil

Highlights

- The temperature response ratios of denitrification potential varied greatly across soils.
- Bacterial rather than fungal denitrification is a key driver for increased denitrification rate under warming.
- Bacterial denitrification showed three-fold higher temperature sensitivity than fungal.

* Correspondence: Yong Li (liyongcn@zju.edu.cn); Di Wu (wudi@iae.ac.cn)

Full list of author information is available at the end of the article.

https://doi.org/10.48130/nc-0026-0004

Graphical abstract

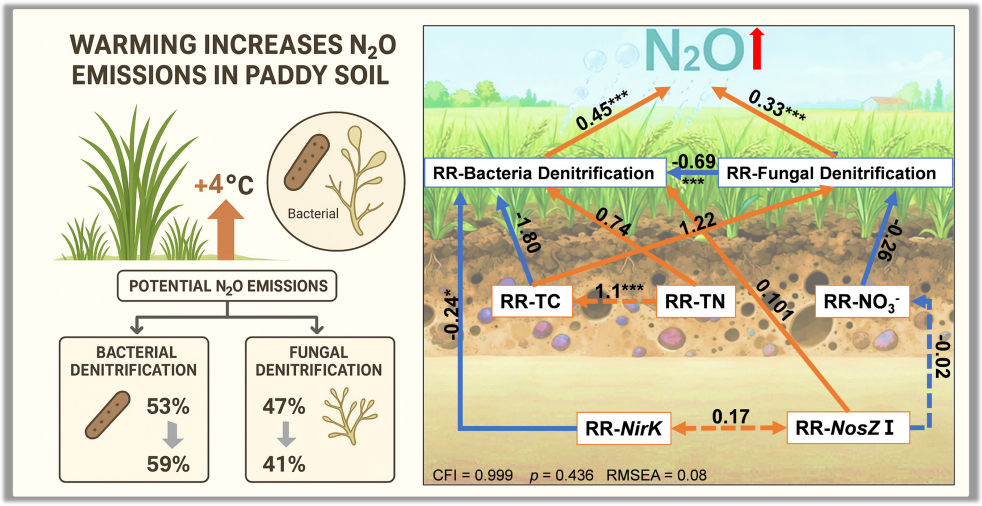

Introduction

Denitrification converts nitrate (NO_3^-) to dinitrogen (N_2) via intermediate nitrogen oxides such as nitrite (NO_2^-), nitric oxide (NO), and nitrous oxide (N_2O), representing a major pathway for N_2O production in anaerobic or redox-dynamic environments[1]. Denitrification in soils was once believed to be predominantly carried out by heterotrophic bacteria, but recent studies showed that fungi also play a significant role[2,3]. Bacterial denitrifiers utilize a suite of enzymes encoded by genes such as *nirK, nirS,* and *nosZ*, which determine the completeness of denitrification, and the N_2O/N_2 product ratio[4,5]. Notably, the distinction between *nirK* and *nirS* has revealed functional and ecological differences among denitrifying bacteria. For instance, *nirK* is often associated with more efficient nitrate-to-N_2O conversion under fluctuating oxygen conditions, while *nirS* may dominate in stable anaerobic environments[6]. Furthermore, the *nosZ* gene is critical for the final step of N_2O reduction to N_2, and its absence or low abundance in certain bacterial communities can lead to elevated N_2O emissions[7]. Recent metagenomic and transcriptomic studies have also identified novel bacterial lineages, such as Thauera and Pseudomonas, as key players in denitrification across diverse soil ecosystems[8]. Additionally, environmental factors like soil moisture, temperature, and nitrate availability have been shown to regulate the expression and activity of these genes, highlighting the dynamic nature of bacterial denitrification[9,10]. Unlike bacteria, fungal denitrifiers often lack the *nosZ* gene equivalent, which limits their ability to complete the reduction of N_2O to N_2, and results in higher N_2O yields as a terminal product[11]. Studies have identified several fungal genera, including Trichoderma, Aspergillus, and Penicillium as active denitrifiers under anaerobic conditions[12]. The role of fungi is particularly pronounced in acidic soils or those with high organic matter content, where they may outcompete bacteria due to their tolerance to low pH, and their ability to utilize complex organic substrates[2,3]. Recent research also suggests that fungal denitrification is driving N_2O emissions, especially in environments dominated by acidic, organic-rich soils[13,14]. Moreover, the interplay between fungal and bacterial denitrifiers under fluctuating redox conditions, such as paddy soil, remains an active area of investigation, with some studies indicating potential synergistic or competitive interactions that modulate overall N_2O production[15].

Future climate projections indicate an increase of approximately 1.5 to 4°C in global mean temperature by the end of the century, with cascading effects on soil biogeochemical cycles[16]. Elevated temperatures can accelerate microbial metabolism, enzyme kinetics, and substrate diffusion, potentially enhancing denitrification rates and N_2O emissions[17,18]. Previous studies have shown inconsistent effects of warming on denitrification potential, while the drivers behind such variations remain unclear[19–21]. The different responses of denitrification rate to warming might be explained by the fundamentally different thermal tolerances and physiological responses of bacterial and fungal denitrifier communities[22]. Bacterial denitrifiers typically exhibit optimal activity within a moderate range (20–30 °C), with rates often doubling or tripling for every 10 °C increase within this window, but their growth and activity can be strongly inhibited as temperatures approach 40 °C[23]. In contrast, fungal denitrifiers, particularly those with *nirK*-type genes, demonstrate greater thermal tolerance, maintaining growth and contributing to N_2O production even at elevated temperatures (e.g., 40 °C) where bacterial activity declines[23]. While bacteria may respond positively to warming through upregulated gene expression (e.g., *nirK* and *nosZ*), fungi may exhibit contrasting patterns due to their broader temperature optima or sensitivity to pH shifts[24]. Warming has been shown to increase fungal α-diversity, while decreasing bacterial richness, potentially shifting community structure and N_2O emissions through changes in soil pH, moisture, and plant interactions[25]. It has been found that warming suppresses abundant fungal taxa and increases bacterial relative dominance, which could reduce overall soil multifunctionality, including nitrogen cycling[26].

Distinguishing the respective roles of bacterial and fungal denitrification is essential for reliably estimating soil N_2O emissions. One commonly used approach for separating these microbial contributions is substrate-induced respiration with selective inhibition (SIRIN)[27]. The SIRIN method has been used to quantify bacterial and fungal denitrification due to its simplicity, low cost, and rapid assessment capabilities in many studies[28]. However, the method faces significant limitations, including inefficient inhibition across different soil types[29]. These non-specific inhibitor effects may affect non-target microbial groups or be metabolized by resistant organisms, leading to inaccurate partitioning of bacterial and fungal contributions[30].

Recent methodological developments in isotope-ratio mass spectrometry and quantum-cascade laser absorption spectroscopy have enabled highly precise determination of intramolecular ^{15}N positioning within the asymmetric N_2O molecule. A key parameter, the ^{15}N site preference (SP), calculated as the difference between $\delta^{15}N$ of the central alpha (α) position, and the terminal beta (β) position ($\delta^{15}N\alpha$–$\delta^{15}N\beta$), has emerged as an effective tracer for differentiating bacterial- and fungal-derived denitrification. N_2O originating from fungal denitrification exhibits consistently high SP values (around 33‰–37‰), while bacterial denitrification yields lower SP values (typically –7.5‰ to +3.5‰, or 0–10‰ depending on the process)[31,32]. This clear isotopic separation makes the SP framework a robust tool for estimating fungal contributions to N_2O emissions across varying environmental conditions[33].

Paddy soils serve as hotspots for N_2O production due to frequent flooding, which create anaerobic conditions conducive to denitrification[34]. Rice paddies contribute an estimated 10%–20% of agricultural N_2O emissions, with denitrification accounting for up to 80% of these under waterlogged regimes[35,36]. The alternating wet-dry cycles in paddy management further enhance N_2O fluxes by promoting coupled nitrification-denitrification, where ammonium oxidation supplies nitrate for subsequent reduction[37]. Warming may exacerbate N_2O production by altering redox potentials, increasing organic carbon mineralization, and shifting microbial community structures in paddy ecosystems[38,39]. However, some studies report increased denitrification under short-term warming due to enhanced microbial activity, while others note declines in long-term scenarios from substrate depletion or community adaptation[40]. Furthermore, most research has focused on overall denitrification-derived N_2O emissions, with limited attention to the differential temperature sensitivities of bacterial vs fungal denitrifiers[41,42].

Using paddy soils collected from multiple locations, this study explored the response of potential denitrification-derived N_2O emissions to warming, and applied the N_2O SP approach to partition fungal and bacterial sources. We hypothesize that bacterial and fungal denitrification will respond differently to warming, driven by interactions between soil nutrients and functional gene abundances. Our findings are expected to advance understanding of microbial controls on N_2O production.

Materials and methods

Study sites and soil properties

Soil samples (0–20 cm) were collected from 18 rice paddies distributed across six provinces in China, extending along a latitudinal gradient from 19°53′ N to 45°31′ N (Supplementary Fig. S1). The selected sites span temperate, subtropical, and tropical monsoon climates, covering a wide variety of agricultural environments. Within each province, three replicate samples were collected from a single representative paddy field. The exact geographical coordinates, mean annual temperature and precipitation, and soil texture of each site are provided in Supplementary Table S1. Additional physicochemical properties (pH, TN, SOC, NH_4^+-N, NO_3^--N) are shown in Supplementary Table S2. Visible plant materials were removed from the collected soils, which were then sieved to 2 mm. Depending on the analysis type, soil was stored at 4 °C (for slurry assays), –20 °C (DNA work), or air-dried (for chemical analysis).

Soil physicochemical properties were characterized using standard analytical procedures. Particle-size distribution was determined by the hydrometer method[43]. Inorganic nitrogen fractions, including NO_3^--N, and NH_4^+-N were analyzed with a continuous-flow autoanalyzer. Soil pH was measured potentiometrically in a 1:2.5 (w/v) soil–water suspension using a calibrated glass electrode (PHS-3C mv/pH meter, Shanghai, China). Dissolved organic carbon (DOC) and dissolved organic nitrogen (DON) were quantified by ultraviolet persulfate oxidation with a total organic carbon analyzer (Phoenix 8000, Teledyne-Tekmar, USA). Available phosphorus concentrations were determined by inductively coupled plasma optical emission spectrometry (ICP-OES; Thermo Fisher, USA). For elemental analysis, soil samples were first finely ground with a ball mill, after which total carbon (TC) and total nitrogen (TN) were measured using an elemental analyzer (Elementar, Germany). Denitrification potential rate (DPR) was assessed using the acetylene inhibition technique[44].

Microcosm construction

Two incubation temperatures were applied in the microcosm experiment: the local average annual temperature of each sampling site (AT), and a warming treatment of +4 °C relative to AT, (ET) (Supplementary Table S3). A +4 °C warming treatment relative to the local mean annual temperature was implemented to represent end-of-century high-emission projections (RCP 8.5, ~3–5 °C regional increase)[45]. In the initial phase, 10 g (oven-dry weight equivalent) of fresh soil was transferred into 50 mL glass incubation vials. Samples were incubated in darkness under two thermal regimes: ambient temperature (AT), and elevated temperature (ET). Throughout the 28-d incubation period, soil moisture was adjusted and maintained at 100% water-filled pore space (WFPS). This process was conducted to eliminate the disturbances to microbial activity caused by sampling and rewetting, and to re-establish a stable background activity level suitable for subsequent denitrification measurements. During the 28-d aerobic preincubation under flooded conditions (100% WFPS), jars were sealed with punctured Parafilm to allow gas exchange with the atmosphere while minimizing evaporative water loss, thereby preventing the buildup of respiratory gases in the headspace.

The second phase, soils were maintained at 100% WFPS and incubated for 48 h following the addition of $NaNO_3$ (0.2 mg) and glucose (1 mg C g^{-1}) as N and C sources. Acetylene (C_2H_2) (final concentration 10% v/v) was applied to the headspace at incubation initiation to block N_2O reduction to N_2. Although the acetylene inhibition technique has known limitations, these were minimized here by anaerobic conditions, a short-term incubation, and continuous slurry shaking. Anaerobic conditions in the incubation bottles were established by flushing with helium gas, and the incubation was conducted at 25 °C. This design enabled comparisons of N_2O production and reduction processes among soils from different regions, particularly along latitudinal gradients. Soil samples were obtained at 0 and 48 h for inorganic N analysis (NO_3^--N and NH_4^+-N). Following 48 h incubation, N_2O concentrations were determined by gas chromatography, and isotopic analyses were performed to derive SP values and assess N_2O formation pathways[31]. Additional subsamples were collected for DNA extraction, functional gene quantification, and microbial community analysis.

Nucleic acid extraction and qPCR

Genomic DNA was extracted from 0.5 g of soil using a spin column-based kit (MP Biomedicals). DNA integrity was assessed by agarose gel electrophoresis, and concentrations and purity were quantified with a Nanodrop® ND-2000 UV–vis spectrophotometer. Quantitative PCR targeting denitrification-associated genes (*nirS*, *nirK*, *FnirK*, *nosZ* I, and *nosZ* II) was conducted on a LightCycler® 480II (Roche, Germany). Primer sequences and cycling conditions are detailed in

https://doi.org/10.48130/nc-0026-0004

Supplementary Table S4. All assays showed acceptable amplification efficiencies (92%–104%), and high R^2 values (0.991–0.999).

SP approach

Following incubation, 12 mL headspace samples were collected into evacuated exetainers (Labco) and analyzed for N_2O isotopocules by IRMS (Delta V Plus, Thermo Fisher Scientific). Molecular N_2O^+ (m/z: 44/45/46) and the fragment NO^+ (m/z: 30/31) ion signals were used to derive isotopic ratios. A laboratory-characterized high-purity N_2O standard (99.995%; Thünen Institute of Climate-Smart Agriculture) was applied as the internal reference, and SP values were obtained via two-point calibration using certified standards[46].

$$\delta^{15}N^{i}\,(‰) = \left(\frac{^{15}N^{i}_{sample}}{^{15}N_{standard}} - 1\right)(i = bulk, \alpha, or\ \beta) \quad (1)$$

$$\delta^{18}O\,(‰) = \frac{^{18}O_{sample}}{^{18}O_{standard}} - 1 \quad (2)$$

$$\delta^{15}N^{bulk}\,(‰) = \frac{\delta^{15}N^{\alpha} + \delta^{15}N^{\beta}}{2} \quad (3)$$

where, $^{15}N^{i}$ and ^{18}O, respectively, denote the isotope ratios of $^{15}N/^{14}N$ and $^{18}O/^{16}O$. $^{15}N^{\alpha}$ and $^{15}N^{\beta}$ are the ratios of $^{15}N/^{14}N$ at the center (^{14}N-^{15}N-^{16}O), and the edge (^{15}N-^{14}N-^{16}O) sites in the N_2O molecule, respectively. Isotopic compositions were expressed in ‰ relative to the Vienna Standard Mean Ocean Water for ^{18}O and atmospheric N_2 for ^{15}N. The SP value of N_2O was defined as:

$$N_2OSP\,(‰) = \delta^{15}N^{\alpha} - \delta^{15}N^{\beta} \quad (4)$$

Analytical precision was approximately 0.3‰, 0.9‰, 0.9‰, and 0.6‰ for $\delta^{15}N^{bulk}$, $\delta^{15}N^{\alpha}$, $\delta^{15}N^{\beta}$, and $\delta^{18}O$, respectively.

Fungal contributions to N_2O production (fFD) were quantified using a two-end-member isotope mixing model[47], assuming bacterial (BD) and fungal (FD) denitrification as the only N_2O sources. The observed ^{15}N site preference (SP_0) of N_2O was used to partition relative pathway contributions, following the mixing balance equation:

$$SP_0 = f_{FD} \times SP_{FD} + f_{BD} \times SP_{BD} \quad (5)$$

where, f_{FD} and f_{BD} represent the fractional contributions of fungal and bacterial denitrification, with SP_{FD} and SP_{BD} denoting their respective SP end-member signatures. A two-source mass balance assumption ($f_{FD} + f_{BD} = 1$) was applied. End-member SP values were set at 37‰ (fungal) and −5‰ (bacterial)[48].

Calculations and statistical analysis

Warming effects on the measured variables were quantified using the response ratio (RR), defined as the natural logarithm (ln) of the mean value under the warming treatment ($\overline{X_t}$) divided by that of the control ($\overline{X_c}$), Eq. (6)[49,50].

$$RR = \ln\left(\frac{\overline{X_t}}{\overline{X_c}}\right) = \ln\left(\overline{X_t}\right) - \ln\left(\overline{X_c}\right) \quad (6)$$

Differences among treatments were analyzed using one-way ANOVA with Tukey's post hoc test, with significance defined at $p < 0.05$. Linear fitting analyses were conducted in OriginPro 2021b. Linear fitting analyses were performed using OriginPro 2021b. Pearson correlation analyses were performed to examine relationships between variations in N_2O emissions, and abiotic as well as biological variables. Structural equation modeling (SEM) was used to quantify direct and indirect effects of key predictors on the N_2O warming RR. Model fit was evaluated using p (> 0.05), CFI (> 0.9), and RMSEA (< 0.008). Statistical analyses were performed in R software (version 4.5.1).

Results

Warming response of denitrification-derived N_2O

The impact of a +4°C warming treatment on denitrification processes was assessed across six Chinese provinces: Heilongjiang (Hj), Shandong (Sd), Jiangsu (Js), Zhejiang (Zj), Guangdong (Gd), and Hainan (Hn). Potential denitrification rates (Fig. 1a) under warming conditions (eT) increased relative to ambient conditions (aT), with mean values of 173.40 μg kg^{-1} h^{-1} (+4%) for Hj, 336.73 μg kg^{-1} h^{-1} (+9%) for Sd, 268.59 μg kg^{-1} h^{-1} (+7%) for Js, 106.32 μg kg^{-1} h^{-1} (+12%) for Zj, 323.24 μg kg^{-1} h^{-1} (+7%) for Gd, and 277.77 μg kg^{-1} h^{-1} (+23%) for Hn. Significant differences between warming and ambient conditions were noted for Sd, Js, Zj, Gd, and Hn ($p < 0.01$). Bacterial denitrification rates (Fig. 1b) under warming conditions were 66.25 μg kg^{-1} h^{-1} (–12%) for Hj, 190.87 μg kg^{-1} h^{-1} (+21%) for Sd, 174.08 μg kg^{-1} h^{-1} (+26%) for Js, 60.91 μg kg^{-1} h^{-1} (+39%) for Zj, 233.29 μg kg^{-1} h^{-1} (+16%) for Gd, and 182.84 μg kg^{-1} h^{-1} (+47%) for Hn, with significant differences for Sd, Js, Gd, and Hn ($p < 0.05$). Fungal denitrification rates (Fig. 1c) under warming conditions were 107.15 μg kg^{-1} h^{-1} for Hj, 145.87 μg kg^{-1} h^{-1} for Sd, 94.513 μg kg^{-1} h^{-1} for Js, 45.416 μg kg^{-1} h^{-1} for Zj, 89.95 μg kg^{-1} h^{-1} for Gd, and 94.93 μg kg^{-1} h^{-1} for Hn, with no significant differences across provinces ($p > 0.01$).

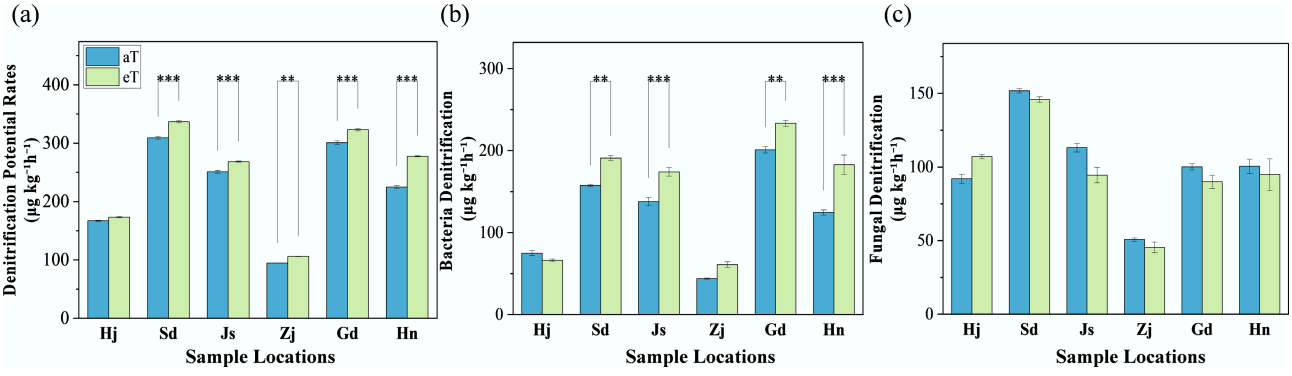

Fig. 1 Response of local denitrification potential rates to warming. Three replicates of one soil sample were used for warming incubations. 'aT' represents the local average annual temperature, and 'eT' represents the elevated temperature (+4 °C), based on the average annual temperature. Sample locations: Heilongjiang (Hj), Shandong (Sd), Jiangsu (Js), Zhejiang (Zj), Guangdong (Gd), and Hainan (Hn). The level of significance is determined by a two-sided *t*-test; * $p < 0.05$, ** $p < 0.01$, and *** $p < 0.001$.

N_2O SP reflects the isotopic composition at specific molecular sites and is used to estimate the relative contributions of bacterial and fungal denitrification[48]. Under ambient conditions (aT), SP values (Fig. 2a) were 18.39‰ for Hj, 14.50‰ for Sd, 16.03‰ for Js, 19.84‰ for Zj, 16.98‰ for Gd, and 16.52‰ for Hn, decreasing by 10%, 15%, 27%, 29%, 39%, and 23%, respectively, under warming conditions (eT). Significant reductions in SP were observed for Js, Zj, and Gd ($p < 0.05$). The relative contributions of denitrification processes (Fig. 2b) under ambient conditions (aT) showed bacterial denitrification at 53.2% and fungal denitrification at 46.8%, with a 6% increase in bacterial contribution under warming conditions (eT).

Response ratios of denitrification-derived N_2O to warming

The RR for potential N_2O denitrification rates to warming was 0.1 (Fig. 3a), while bacterial denitrification exhibited a higher RR of 0.19, and fungal denitrification showed a negative RR of –0.06. The temperature response ratios for fungal denitrification (RR-FD) across all locations (Fig. 3b) displayed no significant differences ($p > 0.05$). In contrast, the bacterial denitrification response ratio (RR-BD) for Hj was significantly lower than that of other locations ($p < 0.05$). These RRs were used to quantify the sensitivity of denitrification processes to warming.

A +4 °C warming treatment elicited varied responses in soil abiotic and biotic factors across six Chinese provinces, with most properties remaining stable but select nutrients and denitrifying genes showing province-specific shifts ($p < 0.05$). Among soil properties, total carbon (TC: 0.89%–3.43%), total nitrogen (TN: 0.09%–0.17%), dissolved organic nitrogen (DON: 14.65–52.62 mg kg^{-1}), nitrate nitrogen (NO_3^--N: 4.38–8.34 mg kg^{-1}), and pH (4.40–7.65) exhibited no consistent warming-induced changes ($p > 0.05$). Dissolved organic carbon (DOC: 25.78–184.97 mg kg^{-1}) decreased significantly only in Hainan, while ammonium nitrogen (NH_4^+-N: 0.20–5.52 mg kg^{-1}) increased significantly only in Shandong (Supplementary Fig. S2).

Denitrifying gene abundances spanned several orders of magnitude and displayed gene- and province-specific responses to warming. Bacterial *nirK* (6.68–18.40 × 10^8 copies g^{-1}) increased by 24% in Heilongjiang, but decreased by 26%–57% in Shandong and Hainan ($p < 0.05$); *nirS* (16.43–55.23 × 10^6 copies g^{-1}) surged 88% in Shandong ($p < 0.001$). Fungal *fnirK* (2.01–54.60 × 10^3 copies g^{-1}), and N_2O-reductase *nosZ I* (0.39–1.35 × 10^8 copies g^{-1}) showed no systematic warming effects ($p > 0.05$), whereas *nosZ II* (0.48–2.63 × 10^8 copies g^{-1}) declined 27.5% in Shandong ($p < 0.05$) (Fig. 4). These selective shifts highlight localized microbial and substrate feedback to warming that likely modulate denitrification-derived N_2O emissions.

Factors driving increased denitrification-derived N_2O under warming

Pearson correlation analysis revealed distinct regulatory patterns for bacterial vs fungal denitrification under warming (Supplementary

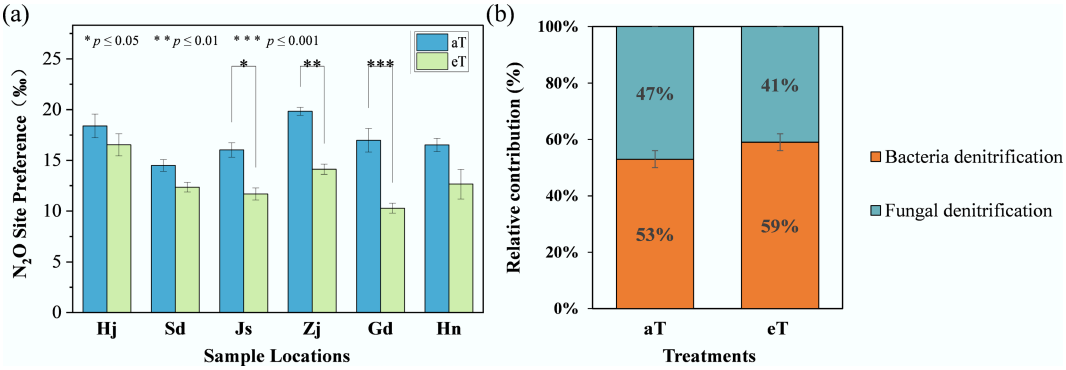

Fig. 2 (**a**) Response of local SP value to warming. (**b**) Relative contributions of bacterial and fungal denitrification. Three replicates of one soil sample were used for warming incubations. The level of significance is determined by two-sided *t*-test; * $p < 0.05$, ** $p < 0.01$, and *** $p < 0.001$.

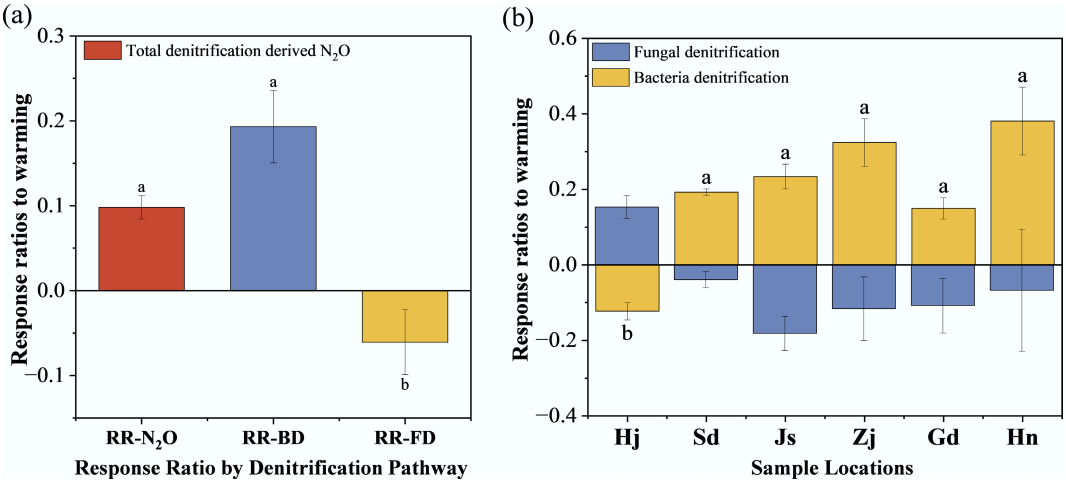

Fig. 3 (**a**), (**b**) Response ratios to warming. Different lowercase letters denote statistically significant differences ($p < 0.05$, Tukey's HSD test).

https://doi.org/10.48130/nc-0026-0004

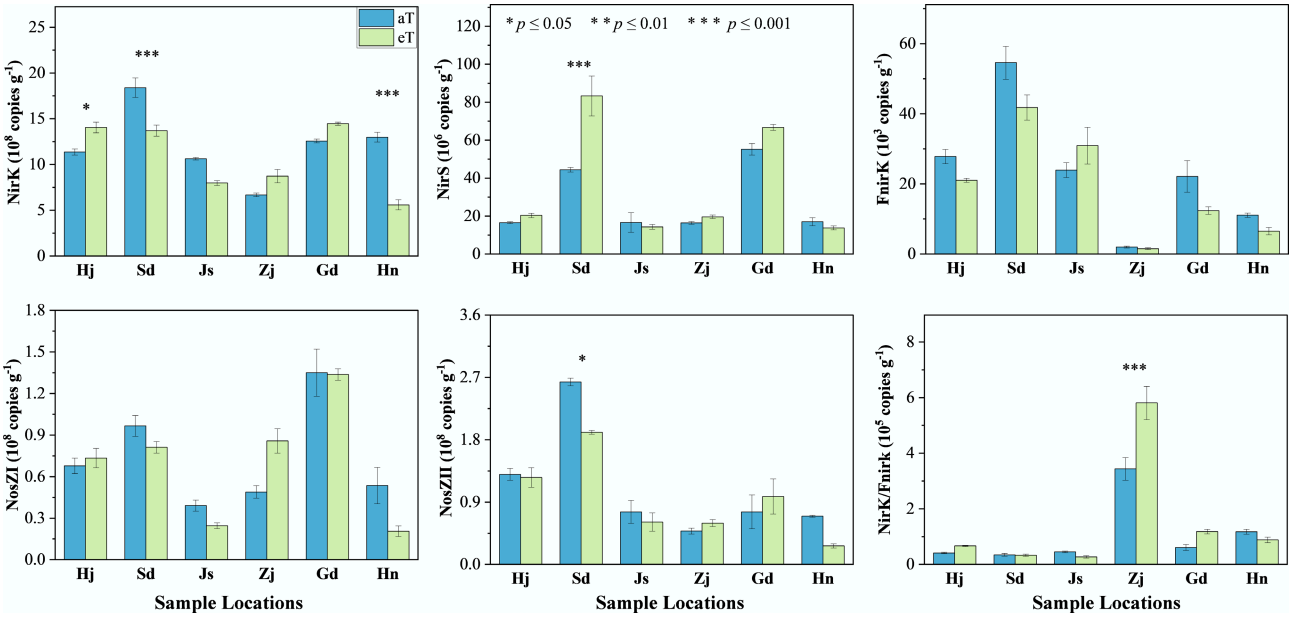

Fig. 4 Effects of warming on the abundance of denitrification function genes at different sampling sites. Three replicates of one soil sample were used for warming incubations. The level of significance is determined by two-sided *t*-test; * $p < 0.05$, ** $p < 0.01$, and *** $p < 0.001$.

Fig. S3). RR-N_2O was negatively correlated with NH_4^+-N ($p < 0.05$), *FnirK* ($p < 0.05$), *nirK* ($p < 0.001$), and *nosZII* ($p < 0.05$). RR-BD was strongly negatively correlated with DOC ($p < 0.05$), DON ($p < 0.05$), NH_4^+-N ($p < 0.001$), *nirK* ($p < 0.001$), and *nosZII* ($p < 0.05$). In contrast, RR-FD was positively correlated with DON ($p < 0.05$) and NH_4^+-N ($p < 0.05$). Potential denitrification rate (N_2O) was strongly positively correlated with RR-BD ($p < 0.001$), RR-FD ($p < 0.001$), pH ($p < 0.05$), *nirS* ($p < 0.01$), and *FnirK* ($p < 0.05$), but strongly negatively correlated with DOC ($p < 0.001$) and DON ($p < 0.001$). Bacterial denitrification rate was negatively correlated with DOC ($p < 0.001$), DON ($p < 0.001$), and NH_4^+-N ($p < 0.05$), and positively correlated with *nirS* ($p < 0.05$). Fungal denitrification rate was positively correlated with clay content ($p < 0.05$), pH ($p < 0.001$), TC ($p < 0.05$), *nirS* ($p < 0.05$), *FnirK* ($p < 0.001$), and *nosZII* ($p < 0.001$).

The relationships between the response ratios of potential N_2O denitrification rates (RR-N_2O) and RR of various factors were explored using a correlation heatmap (Fig. 5). RR-N_2O exhibited a significant positive correlation with RR-BD and the response ratio of ammonium nitrogen (RR-NH_4^+) ($p < 0.05$), while showing significant negative correlations with the response ratios of dissolved organic carbon (RR-DOC) and the *nirK* gene (RR-nirK) ($p < 0.05$). Additionally, RR-BD was significantly negatively correlated with RR-nirK and the response ratio of total carbon (RR-TC) ($p < 0.05$). Regression analysis revealed that RR-N_2O increased significantly with rising RR-BD (r^2 = 0.47, $p < 0.001$) (Fig. 6a). In contrast, no significant influence was observed from changes in the RR-FD (Fig. 6b). Additionally, regression analysis revealed a significant negative effect of RR-BD on RR-FD ($r^2 = 0.566$, $p < 0.001$) (Fig. 6c).

The SEM analysis (Fig. 7) elucidated the direct and indirect effects of a +4°C warming treatment on N_2O emissions, integrating RR of biotic and abiotic factors. The model demonstrated a good fit, with a Comparative Fit Index (CFI) of 0.999, a root mean square error of approximation (RMSEA) of 0.008, and a standardized root mean square residual (SRMR) of 0.071, indicating robust explanatory power ($p = 0.436$). The increase in N_2O emissions induced by warming was positively regulated by the RR-BD (path coefficient = 0.45, $p < 0.001$) and RR-FD (path coefficient = 0.33, $p < 0.001$). RR-BD was significantly influenced by RR-nirK (path coefficient = −0.242) and RR-total nitrogen (RR-TN) (path coefficient = 0.740), though only the negative relationship with RR-nirK was significant ($p < 0.05$). Additionally, RR-BD and RR-FD exhibited a significant negative correlation (path coefficient = −0.69, $p < 0.001$), reflecting a trade-off between bacterial and fungal denitrification under warming. RR-N_2O was indirectly negatively influenced by RR-nirK through RR-BD (path coefficient = −0.242, $p < 0.05$). These findings highlight the complex

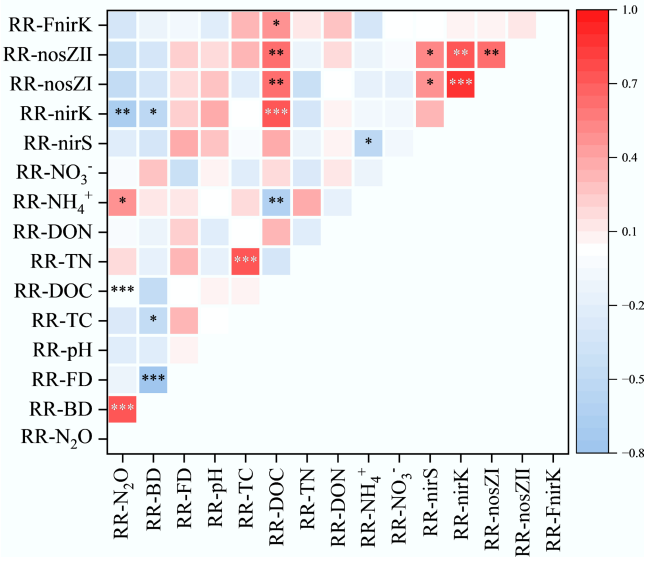

Fig. 5 Pearson correlation analysis between climate factors, soil properties, functional gene abundance, N_2O production rates, and their response ratios. The correlation coefficients ranging from negative to positive are indicated by colour gradient from red to blue. The level of significance is determined by two-sided *t*-test; * $p < 0.05$, ** $p < 0.01$, and *** $p < 0.001$.

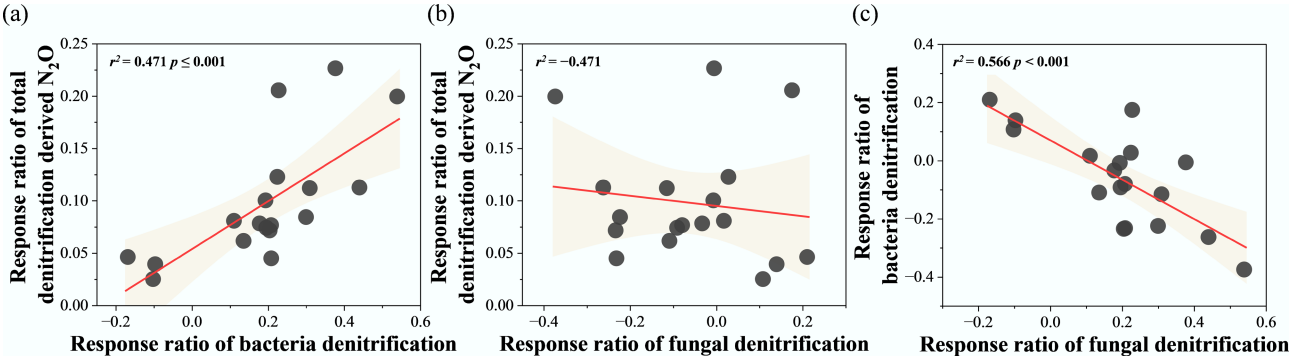

Fig. 6 Regression analysis between response ratio of total denitrification derived N_2O (RR-N_2O), response ratio of bacterial denitrification (RR-BD), and response ratio of fungal denitrification (RR-FD). * $p < 0.05$, ** $p < 0.01$, and *** $p < 0.001$.

interplay of soil properties and microbial processes in driving warming-induced N_2O emissions.

Discussion

Our findings showed that a +4 °C warming treatment generally enhanced potential denitrification rates in paddy soils, with increases varying from 4% to 23% across different soil types. This aligns with previous meta-analyses showing that warming increased global terrestrial N_2O emissions by an average of 33% across all biomes, with particularly strong responses in warmer cropland regions, primarily due to accelerated microbial activity and enhanced substrate availability under elevated temperatures[51,52]. In our study, soil collected in the tropical climate province (Hainan) exhibited the highest increase in total denitrification (+23%). In contrast, soil collected in Heilongjiang, a northern province characterized by colder ambient conditions, showed a relatively modest increase (+4%). This is likely because bacterial communities in colder regions tend to be less responsive to temperature changes, exhibiting lower temperature sensitivity than those in warmer climates[53]. This regional disparity highlights the need for latitude-specific models to predict N_2O responses, as southern provinces (e.g., Hainan, with a 23% potential rate increase) may experience amplified emissions due to year-round warm conditions that facilitate continuous denitrification cycles[54].

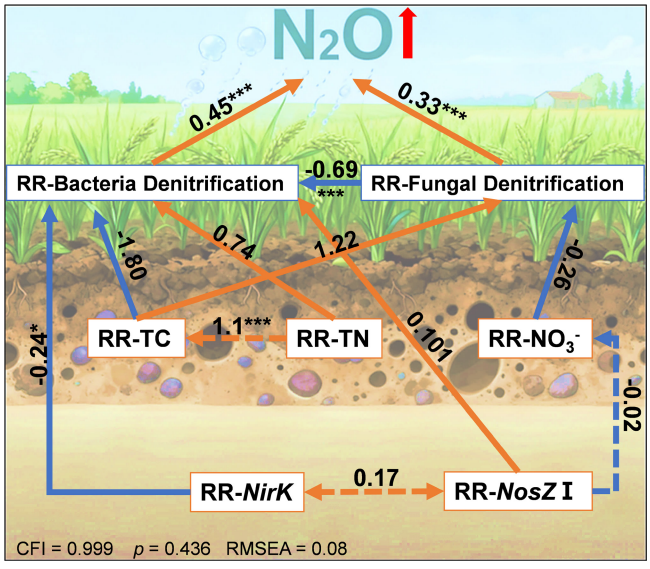

Fig. 7 Structural equation models illustrating the direct and indirect effects of selected variables on response ratios of RR-N_2O. Red and blue arrows indicate positive and negative effects, respectively. Solid and dashed lines represent significant and nonsignificant paths, respectively. Numbers next to the arrows are standardized path coefficients (* $p < 0.05$, ** $p < 0.01$, and *** $p < 0.001$).

In our study, the contrasting responses of bacterial and fungal denitrification to warming underscore the functional divergence within microbial guilds. Bacterial denitrification rates increased significantly in four out of six provinces under +4°C warming. This is consistent with findings that bacteria tend to exhibit greater temperature sensitivity in short-term studies, possibly due to their generally higher metabolic rates and faster growth responses to warming[53,55]. In contrast, fungal denitrification showed no significant response to warming ($p > 0.01$), with RRs averaging −0.06, suggesting that fungi, often more resilient to environmental perturbations through spore formation and broader pH tolerance, are less temperature-sensitive in N_2O production[56]. It has been suggested that fungi may not respond as acutely to short-term warming due to their slower growth kinetics and reliance on complex organic substrates[12,57]. The asymmetric sensitivities of bacterial and fungal denitrifiers may stem from bacteria's higher temperature-sensitivity coefficient for denitrification enzymes like nitrite reductase (*nirK*/*nirS*) compared to fungal counterparts (*fnirK*)[1]. This differential response implies a potential shift in microbial community dominance under future climate scenarios, where bacterial pathways could disproportionately contribute to N_2O fluxes, exacerbating greenhouse gas emissions in bacterial denitrification-dominant soil conditions.

The significant positive correlation between RR-N_2O and RR-BD suggests that the response of potential denitrification rate to warming is predominantly controlled by bacterial denitrification (Fig. 5). Regression models further confirmed that RR-N_2O rises linearly with RR-BD ($r^2 = 0.47$, $p < 0.001$), but not RR-FD, emphasizing bacterial dominance in warming responses. The structural equation model (SEM) further elucidates these dynamics, with a robust fit (CFI = 0.999, RMSEA = 0.008, SRMR = 0.071) revealing positive direct effects of RR-BD (path coefficient = 0.45, $p < 0.001$) and RR-FD (0.33, $p < 0.001$) on RR-N_2O, but also highlighting trade-offs between bacterial and fungal denitrification (path coefficient = −0.69, $p < 0.001$). This trade-off may arise from differences in resource allocation, where bacteria invest in rapid, specialized denitrification pathways for higher energy yield under fluctuating conditions, while fungi prioritize metabolic flexibility, leading to niche partitioning in complex soils[58,59]. Additionally, regression analysis revealed a

significant negative effect of RR-BD on RR-FD (r^2 = 0.566, p < 0.001) (Fig. 6c), indicating a competitive interaction where enhanced bacterial activity under warming may suppress fungal denitrification. This competitive suppression likely stems from resource competition, as bacteria exploit labile carbon and nitrogen substrates more efficiently at elevated temperatures, reducing availability to fungi[15]. These findings imply that warming could amplify N_2O emissions more profoundly in subtropical and tropical soils, where bacterial denitrifiers thrive, posing risks to N budgets in rice-paddy-dominated regions. Globally, rice paddies are predominantly located in subtropical and tropical regions, such as South and Southeast Asia, where warm, humid conditions support year-round rice cultivation and continuous denitrification cycles. An indirect negative effect of RR-nirK on RR-N_2O via RR-BD (−0.242, p < 0.05) was also found, indicating that warming may suppress *nirK*-type denitrifiers, potentially reducing N_2O production efficiency despite overall rate increases[60,61].

In paddy soils under elevated temperatures, the inter-relationships between bacterial and fungal communities can significantly influence denitrification processes through complex co-occurrence networks that modulate N_2O production and consumption pathways[62]. It has been found that fungal denitrifiers dominate N_2O emissions in flooded paddy soils with lower organic carbon content, contributing 58%–77% to net emissions, while bacterial denitrifiers account for only 6%–15%, indicating competitive dynamics under anoxic conditions[63]. These interactions are further evidenced by positive and negative associations in microbial networks, with higher connectivity among *nirS*-, *nirK*-, and fungal nirK-containing taxa potentially enhancing overall denitrification efficiency and affecting N_2O flux in response to soil properties such as pH and organic matter[64]. Warming exacerbates these bacterial-fungal dynamics by shifting denitrifier community structures, particularly sensitizing *nirS*-type bacterial denitrifiers, which may indirectly amplify fungal contributions to N_2O emissions in paddy systems[61]. Overall, these microbial interactions explain a substantial portion of the variance in N_2O emissions and their temperature sensitivity in rice paddy fields. While our short-term incubation experiment provides insights into immediate microbial responses to warming, it does not fully replicate the gradual temperature increases projected under climate change scenarios, which may allow microbial community acclimation and shift over longer periods. Future studies should employ gradual, long-term field warming to better mimic natural climate change, which may promote greater functional coordination or compensation between bacterial and fungal denitrifiers.

Conclusions

Our findings demonstrate that a +4 °C warming treatment significantly enhances denitrification-derived N_2O emissions in paddy soils, primarily through stimulated bacterial denitrification (mean RR of 0.19), while fungal pathways exhibit minimal sensitivity (mean RR of −0.06). Regression and SEM analyses confirm that bacterial dominance drives N_2O responses (r^2 = 0.47, p < 0.001), alongside a strong competitive trade-off between bacterial and fungal pathways (negative path coefficient: −0.69, p < 0.001). These results highlight that future climate warming may pose a greater risk to the nitrogen budget and greenhouse gas reduction of rice-dominated agricultural ecosystems by enhancing bacterial contributions. However, as a short-term study, our results primarily capture acute physiological responses and may overestimate the warming effects compared to long-term scenarios, in which microbial acclimation, community restructuring, and potential functional compensation or coordination between bacterial and fungal denitrifiers could moderate N_2O fluxes. Future long-term field warming experiments with gradual temperature trajectories are essential to validate these short-term insights and better predict ecosystem feedback.

Supplementary information

It accompanies this paper at: https://doi.org/10.48130/nc-0026-0004.

Author contributions

The authors confirm their contributions to the paper as follows: Lixin Jia: study conception and design, draft manuscript preparation, data analysis, visualization; Yong Li: original research plan, all site and soil experiments; Roland Bol: review and editing; Di Wu: study conception and design, review and editing. All authors reviewed the results and approved the final version of the manuscript.

Data availability

All data generated or analyzed during this study are included in this published article.

Funding

This work was supported by the Shandong Provincial Natural Science Foundation (Grant No. ZR2024YQ039), National Natural Science Foundation of China (Grant No. 42377291), LiaoNing Revitalization Talents Program (Grant No. XLYC2403096), and Natural Science Foundation of Zhejiang Province (Grant No. LR23D010002).

Acknowledgments

The authors thank Chaobiao Meng, Zhejiang University, for his assistance with the incubation experiment.

Declarations

Competing interests

The authors declare no conflict of interest.

Author details

[1]College of Resources and Environmental Sciences, China Agricultural University, Beijing 100193, China; [2]CAS Key Laboratory of Forest Ecology and Silviculture, Key Laboratory of Stable Isotope Techniques and Applications, Institute of Applied Ecology, Chinese Academy of Sciences, Shenyang 110016, China; [3]Zhejiang Provincial Key Laboratory of Agricultural Resources and Environment, State Key Laboratory of Soil Pollution Control and Safety, College of Environmental and Resource Sciences, Zhejiang University, Hangzhou 310058, China; [4]Institute of Bio- and Geosciences, Agrosphere (IBG-3), Forschungszentrum Jülich GmbH, 52425 Jülich, Germany; [5]Environment Centre Wales, Bangor University, Gwynedd, LL57 2UW, UK

References

[1] Butterbach-Bahl K, Baggs EM, Dannenmann M, Kiese R, Zechmeister-Boltenstern S. 2013. Nitrous oxide emissions from soils: how well do we understand the processes and their controls? *Philosophical Transactions of the Royal Society B: Biological Sciences* 368:20130122

[2] Laughlin RJ, Stevens RJ. 2002. Evidence for fungal dominance of denitrification and codenitrification in a grassland soil. *Soil Science Society of America Journal* 66:1540–1548

[3] Shoun H, Fushinobu S, Jiang L, Kim SW, Wakagi T. 2012. Fungal denitrification and nitric oxide reductase cytochrome P450nor. *Philosophical Transactions of the Royal Society B: Biological Sciences* 367:1186–1194

[4] Philippot L, Čuhel J, Saby NPA, Chèneby D, Chroňáková A, et al. 2009. Mapping field-scale spatial patterns of size and activity of the denitrifier community. *Environmental Microbiology* 11:1518–1526

[5] Zumft WG. 1997. Cell biology and molecular basis of denitrification. *Microbiology and Molecular Biology Reviews* 61:533–616

[6] Liang Y, Wu C, Wei X, Liu Y, Chen X, et al. 2021. Characterization of *nirS*- and *nirK*-containing communities and potential denitrification activity in paddy soil from eastern China. *Agriculture, Ecosystems & Environment* 319:107561

[7] Shan J, Sanford RA, Chee-Sanford J, Ooi SK, Löffler FE, et al. 2021. Beyond denitrification: the role of microbial diversity in controlling nitrous oxide reduction and soil nitrous oxide emissions. *Global Change Biology* 27:2669–2683

[8] Hu YQ, Zeng YX, Du Y, Zhao W, Li HR, et al. 2023. Comparative genomic analysis of two Arctic *Pseudomonas* strains reveals insights into the aerobic denitrification in cold environments. *BMC Genomics* 24:534

[9] Giles M, Morley N, Baggs EM, Daniell TJ. 2012. Soil nitrate reducing processes – drivers, mechanisms for spatial variation, and significance for nitrous oxide production. *Frontiers in Microbiology* 3:407

[10] Li Z, Tang Z, Song Z, Chen W, Tian D, et al. 2022. Variations and controlling factors of soil denitrification rate. *Global Change Biology* 28:2133–2145

[11] Maeda K, Spor A, Edel-Hermann V, Heraud C, Breuil MC, et al. 2015. N_2O production, a widespread trait in fungi. *Scientific Reports* 5:9697

[12] Bösch Y, Pold G, Saghaï A, Karlsson M, Jones CM, et al. 2023. Distribution and environmental drivers of fungal denitrifiers in global soils. *Microbiology Spectrum* 11:e00061-23

[13] Ambus P, Zechmeister-Boltenstern S. 2007. Denitrification and N-cycling in forest ecosystems. In *Biology of the Nitrogen Cycle*, eds. Bothe H, Ferguson SJ, Newton WE. Amsterdam: Elsevier. pp. 343–358 doi: 10.1016/b978-044452857-5.50023-0

[14] Jeewani PH, Brown RW, Rhymes JM, Evans CD, Chadwick DR, et al. 2025. Restoring degraded agricultural peatlands: how rewetting, biochar, and iron sulphate synergistically modify microbial hotspots and carbon storage. *Biochar* 7:108

[15] Wang C, Kuzyakov Y. 2024. Mechanisms and implications of bacterial–fungal competition for soil resources. *The ISME Journal* 18:wrae073

[16] Intergovernmental Panel on Climate Change (IPCC). 2023. *Climate change 2022 – impacts, adaptation and vulnerability: Working group II contribution to the sixth assessment report of the intergovernmental panel on climate change*. Cambridge: Cambridge University Press. doi: 10.1017/9781009325844

[17] Abdalla M, Jones M, Ambus P, Williams M. 2010. Emissions of nitrous oxide from Irish arable soils: effects of tillage and reduced N input. *Nutrient Cycling in Agroecosystems* 86:53–65

[18] Greaver TL, Clark CM, Compton JE, Vallano D, Talhelm AF, et al. 2016. Key ecological responses to nitrogen are altered by climate change. *Nature Climate Change* 6:836–843

[19] Cosentino VRN, Figueiro Aureggui SA, Taboada MA. 2013. Hierarchy of factors driving N_2O emissions in non-tilled soils under different crops. *European Journal of Soil Science* 64:550–557

[20] Davidson EA, Janssens IA. 2006. Temperature sensitivity of soil carbon decomposition and feedbacks to climate change. *Nature* 440:165–173

[21] Kim M, Lim HS, Hyun CU, Cho A, Noh HJ, et al. 2019. Local-scale variation of soil bacterial communities in ice-free regions of maritime Antarctica. *Soil Biology and Biochemistry* 133:165–173

[22] Cui P, Fan F, Yin C, Song A, Huang P, et al. 2016. Long-term organic and inorganic fertilization alters temperature sensitivity of potential N_2O emissions and associated microbes. *Soil Biology and Biochemistry* 93:131–141

[23] Xu X, Liu X, Li Y, Ran Y, Liu Y, et al. 2017. High temperatures inhibited the growth of soil bacteria and archaea but not that of fungi and altered nitrous oxide production mechanisms from different nitrogen sources in an acidic soil. *Soil Biology and Biochemistry* 107:168–179

[24] Tan X, Shao D, Gu W. 2018. Effects of temperature and soil moisture on gross nitrification and denitrification rates of a Chinese lowland paddy field soil. *Paddy and Water Environment* 16:687–698

[25] Jiang M, Tian Y, Guo R, Li S, Guo J, et al. 2023. Effects of warming and nitrogen addition on soil fungal and bacterial community structures in a temperate meadow. *Frontiers in Microbiology* 14:1231442

[26] Qiu Y, Zhang K, Zhao Y, Zhao Y, Wang B, et al. 2023. Climate warming suppresses abundant soil fungal taxa and reduces soil carbon efflux in a semi-arid grassland. *mLife* 2:389–400

[27] Anderson JPE, Domsch KH. 1975. Measurement of bacterial and fungal contributions to respiration of selected agricultural and forest soils. *Canadian Journal of Microbiology* 21:314–322

[28] Abbas T, Zhou H, Zhang Q, Li Y, Liang Y, et al. 2019. Anammox co-fungi accompanying denitrifying bacteria are the thieves of the nitrogen cycle in paddy-wheat crop rotated soils. *Environment International* 130:104913

[29] Rohe L, Anderson TH, Flessa H, Goeske A, Lewicka-Szczebak D, et al. 2021. Comparing modified substrate-induced respiration with selective inhibition (SIRIN) and N_2O isotope approaches to estimate fungal contribution to denitrification in three arable soils under anoxic conditions. *Biogeosciences* 18:4629–4650

[30] Keuschnig C, Gorfer M, Li G, Mania D, Frostegård Å, et al. 2020. NO and N_2O transformations of diverse fungi in hypoxia: evidence for anaerobic respiration only in *Fusarium* strains. *Environmental Microbiology* 22:2182–2195

[31] Sutka RL, Ostrom NE, Ostrom PH, Breznak JA, Gandhi H, et al. 2006. Distinguishing nitrous oxide production from nitrification and denitrification on the basis of isotopomer abundances. *Applied and Environmental Microbiology* 72:638–644

[32] Toyoda S, Mutobe H, Yamagishi H, Yoshida N, Tanji Y. 2005. Fractionation of N_2O isotopomers during production by denitrifier. *Soil Biology and Biochemistry* 37:1535–1545

[33] Wu D, Köster JR, Cárdenas LM, Brüggemann N, Lewicka-Szczebak D, et al. 2016. N_2O source partitioning in soils using ^{15}N site preference values corrected for the N_2O reduction effect. *Rapid Communications in Mass Spectrometry* 30:620–626

[34] Kögel-Knabner I, Amelung W, Cao Z, Fiedler S, Frenzel P, et al. 2010. Biogeochemistry of paddy soils. *Geoderma* 157:1–14

[35] Akiyama H, Yagi K, Yan X. 2005. Direct N_2O emissions from rice paddy fields: summary of available data. *Global Biogeochemical Cycles* 19:2004GB002378

[36] Zou J, Huang Y, Zheng X, Wang Y. 2007. Quantifying direct N_2O emissions in paddy fields during rice growing season in mainland China: dependence on water regime. *Atmospheric Environment* 41:8030–8042

[37] Zhu T, Zhang J, Yang W, Cai Z. 2013. Effects of organic material amendment and water content on NO, N_2O, and N_2 emissions in a nitrate-rich vegetable soil. *Biology and Fertility of Soils* 49:153–163

[38] Liu Y, Ge T, Ye J, Liu S, Shibistova O, et al. 2019. Initial utilization of rhizodeposits with rice growth in paddy soils: rhizosphere and N fertilization effects. *Geoderma* 338:30–39

[39] Zhou M, Zhu B, Wang S, Zhu X, Vereecken H, et al. 2017. Stimulation of N_2O emission by manure application to agricultural soils may largely offset carbon benefits: a global meta-analysis. *Global Change Biology* 23:4068–4083

[40] Wang J, Song Y, Ma T, Raza W, Li J, et al. 2017. Impacts of inorganic and organic fertilization treatments on bacterial and fungal communities in a paddy soil. *Applied Soil Ecology* 112:42–50

[41] Jia L, Yang H, Li Y, Du Z, Ju X, et al. 2025. Soil clay content determined the temperature response of N_2O emissions derived from denitrification. *Applied Soil Ecology* 216:106500

[42] Rohe L, Anderson TH, Braker G, Flessa H, Giesemann A, et al. 2014. Dual isotope and isotopomer signatures of nitrous oxide from fungal

denitrification – a pure culture study: isotopomer signatures of N_2O from fungal denitrification. *Rapid Communications in Mass Spectrometry* 28:1893–1903

[43] Gee GW, Bauder JW. 1986. Particle-size analysis. In *Methods of Soil Analysis: Part 1 Physical and Mineralogical Methods*, ed. Klute A. Madison, WI: American Society of Agronomy, Crop Science Society of America, and Soil Science Society of America. pp. 383–411. doi: 10.2136/sssabookser5.1.2ed.c15

[44] Petersen DG, Blazewicz SJ, Firestone M, Herman DJ, Turetsky M, et al. 2012. Abundance of microbial genes associated with nitrogen cycling as indices of biogeochemical process rates across a vegetation gradient in Alaska. *Environmental Microbiology* 14:993–1008

[45] Zhao C, Liu B, Piao S, Wang X, Lobell DB, et al. 2017. Temperature increase reduces global yields of major crops in four independent estimates. *Proceedings of the National Academy of Sciences of the United States of America* 114:9326–9331

[46] Su X, Wen T, Wang Y, Xu J, Cui L, et al. 2021. Stimulation of N_2O emission via bacterial denitrification driven by acidification in estuarine sediments. *Global Change Biology* 27:5564–5579

[47] Ostrom NE, Sutka R, Ostrom PH, Grandy AS, Huizinga KM, et al. 2010. Isotopologue data reveal bacterial denitrification as the primary source of N_2O during a high flux event following cultivation of a native temperate grassland. *Soil Biology and Biochemistry* 42:499–506

[48] Toyoda S, Yoshida N, Koba K. 2017. Isotopocule analysis of biologically produced nitrous oxide in various environments. *Mass Spectrometry Reviews* 36:135–160

[49] Hedges LV, Gurevitch J, Curtis PS. 1999. The meta-analysis of response ratios in experimental ecology. *Ecology* 80:1150–1156

[50] Luo Y, Hui D, Zhang D. 2006. Elevated CO_2 stimulates net accumulations of carbon and nitrogen in land ecosystems: a meta-analysis. *Ecology* 87:53–63

[51] Wang X, Li Ye, Waqas MA, Wang B, Hassan W, et al. 2021. Divergent terrestrial responses of soil N_2O emissions to different levels of elevated CO_2 and temperature. *Oikos* 130:1440–1449

[52] Xu R, Tian H, Pan S, Prior SA, Feng Y, et al. 2020. Global N_2O emissions from cropland driven by nitrogen addition and environmental factors: comparison and uncertainty analysis. *Global Biogeochemical Cycles* 34:e2020GB006698

[53] Rinnan R, Rousk J, Yergeau E, Kowalchuk GA, Bååth E. 2009. Temperature adaptation of soil bacterial communities along an Antarctic climate gradient: predicting responses to climate warming. *Global Change Biology* 15:2615–2625

[54] Ghimire U, Shrestha NK, Biswas A, Wagner-Riddle C, Yang W, et al. 2020. A review of ongoing advancements in soil and water assessment tool (SWAT) for nitrous oxide (N_2O) modeling. *Atmosphere* 11:450

[55] Smith TP, Thomas TJH, García-Carreras B, Sal S, Yvon-Durocher G, et al. 2019. Community-level respiration of prokaryotic microbes may rise with global warming. *Nature Communications* 10:5124

[56] Chen Z, Wang Q, Ma J, Zou P, Yu Q, et al. 2020. Fungal community composition change and heavy metal accumulation in response to the long-term application of anaerobically digested slurry in a paddy soil. *Ecotoxicology and Environmental Safety* 196:110453

[57] Wang H, Li J, Chen H, Liu H, Nie M. 2022. Enzymic moderations of bacterial and fungal communities on short- and long-term warming impacts on soil organic carbon. *Science of The Total Environment* 804:150197

[58] Chen Q, Han F, Lyu M, Zeng Z, Cai Y, et al. 2025. Distinct responses of fungal and bacterial denitrification genes to seasonal changes, nitrogen deposition and precipitation reduction in subtropical forest soils. *Applied Soil Ecology* 213:106322

[59] Roothans N, Van Loosdrecht MCM, Laureni M. 2025. Metabolic labour division trade-offs in denitrifying microbiomes. *The ISME Journal* 19:wraf020

[60] Deng X, Xu T, Zhang F, Xue L, Yang L, et al. 2024. Effects of warming and fertilization on *nirK*-, *nirS*- and *nosZ*-type denitrifier communities in paddy soil. *Science of The Total Environment* 955:177057

[61] Xing XY, Tang YF, Xu HF, Qin HL, Liu Y, et al. 2021. Warming shapes *nirS*- and *nosZ*-type denitrifier communities and stimulates N_2O emission in acidic paddy soil. *Applied and Environmental Microbiology* 87:e02965-20

[62] Xue P, Minasny B, McBratney AB. 2022. Land-use affects soil microbial co-occurrence networks and their putative functions. *Applied Soil Ecology* 169:104184

[63] Tang Y, Minasny B, McBratney A. 2024. Partitioning denitrification pathways in N_2O emissions from re-flooded dry paddy soils. *Biogeochemistry* 167:1315–1333

[64] Xiao X, Delgado-Baquerizo M, Shen H, Ma Z, Zhou J, et al. 2023. Microbial interactions related to N_2O emissions and temperature sensitivity from rice paddy fields. *mBio* 14:e03262-22